

## 스크류원심펌프 임펠러 자오면형상 설계파라미터 최적화

황티홍밍\* · 쩌엥비엣안\*\* · 쉬레스트 우즈왈\* · 최영도\*\*\*†

# Optimization of the Meridional Plane Shape Design Parameters in a Screw Centrifugal Pump Impeller

Thi Hong Minh Hoang\*, Viet Anh Truong\*\*, Ujjwal Shrestha\*, Young-Do Choi\*\*\*†

*Key Words* : Screw centrifugal pump (스크류원심펌프), Pump performance (펌프성능), Impeller meridional plane shape (임펠러 자오면형상), Design parameter (설계파라미터), Optimization (최적화)

### ABSTRACT

Screw centrifugal pump is a non-clog type pump, which is widely used for drainage and sewage control systems. The screw centrifugal pump combines the advantages of the screw pump and centrifugal pump. Screw centrifugal pump shows the relatively high efficiency and the good solids handling capability. Based on a screw centrifugal pump design method, the parameters of impeller meridional plane shape are investigated for the improvement of pump performance. The design parameters of impeller meridional plane shape, such as impeller inlet and outlet diameters, outlet width, total axial length, blade inlet and outlet angles, and inclination angles, were investigated to examine their effects on the pump performance. Numerical analysis was conducted to determine the essential design variables for the screw centrifugal pump. Furthermore, flow passage shape optimization was conducted to enhance the performance of the screw centrifugal pump.

## 1. Introduction

Screw centrifugal pump is a special type of pump, which is a combination of a positive displacement pump (screw pump) and a centrifugal pump. The impeller of this pump includes the screw part having the spiral propeller effect as well as the centrifugal part having the centrifugal effect<sup>(1)</sup>. Therefore, the screw centrifugal pump is inherited many advantages from the screw pump and centrifugal pump, such as hydraulic characteristics, solids handling capability, cavitation resistance and high efficiency.

Recently, some topics related to the screw centrifugal pump is available. Kim *et al.*<sup>(2)</sup> studied the effect of entrained air in a small screw-type

centrifugal pump. The impact of the mean size of bubbles, tip clearances and flow patterns on pump performance was confirmed. Tatebayashi *et al.*<sup>(3)</sup> studied the influence of meridional shape on screw-type centrifugal pump performance. The thrust in the screw-type centrifugal pump was investigated by Tatebayashi *et al.*<sup>(4)</sup>, which showed that the axial thrust became maximum when the impeller radius reached the tongue of the volute casing. Tatebayashi *et al.*<sup>(5)</sup> continuously studied the pump performance improvement by restraining back flow in screw-type centrifugal pump. However, the previous study did not show the specific design method of screw centrifugal pump. Cheng *et al.*<sup>(6)</sup> studied the parameter equation for the screw centrifugal pump impeller blade and Guo

\* Graduate school, Department of Mechanical Engineering, Mokpo National University

\*\* School of Transportation Engineering, Hanoi University of Science and Technology, Hanoi, Vietnam

\*\*\* Department of Mechanical Engineering, Mokpo National University

† Corresponding Author, E-mail : ydchoi@mokpo.ac.kr

*et al.*<sup>(7)</sup> studied the design method and internal flow characteristics of the screw centrifugal pump. These papers are one of the few studies to suggest the clear design method of the screw centrifugal pump impeller. Currently, there is no study to show the optimization of the screw centrifugal pump performance.

In this study, the screw centrifugal pump performance is investigated by changing the design parameters of the impeller meridional plane shape. The Computational Fluid Dynamics (CFD) analysis is conducted to study the effect of the impeller meridional plane shape on the screw centrifugal pump performance. Then, the optimization of the impeller meridional plane shape is performed to improve the pump performance. A numerical code of ANSYS CFX 18.1<sup>(8)</sup> is applied for all numerical simulations.

## 2. Design of Screw Centrifugal Pump

Fig. 1 shows the schematic view of the screw centrifugal pump model<sup>(9)</sup>. The design specification of the screw centrifugal pump model is illustrated in Table 1. The impeller meridional plane shape plays a vital role in screw centrifugal pump performance and is established by the pump parameters, which are

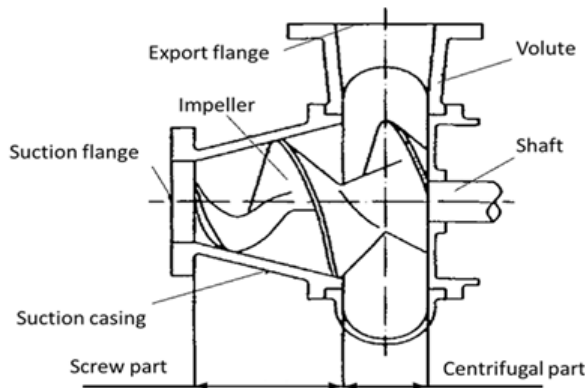


Fig. 1 Schematic view of screw centrifugal pump model (9)

Table 1 Design specification of screw centrifugal pump model

Item	Nomenclature	Value
Flow rate	$Q [m^3/s]$	0.064
Head	$H [m]$	4
Rotational speed	$n [\text{min}^{-1}]$	650
Specific speed	$n_s = \frac{3.65n \sqrt{Q}}{H^{0.75}}$ [ $\text{min}^{-1}, m^3/s, m$ ]	212

calculated by the equations<sup>(4,7)</sup>. The 2D meridional plane shape of the screw centrifugal impeller blade model is shown in Fig. 2. The meridional plane shape consists of the shroud line ( $a_1a_2a_3a_4$ ) including Arc-Line-Line, the hub line ( $b_1b_2b_3b_4$ ) including Arc-Line-Arc, the impeller blade inlet line ( $a_1b_1$ ) including a Line, and the impeller blade outlet line ( $a_4b_4$ ) including a Line. The design parameters listed in Table 2 are used to established the impeller meridional plane shape of the initial model showed in Fig. 2.

The previous studies<sup>(6,7)</sup> showed the detailed design method of the screw centrifugal pump impeller,

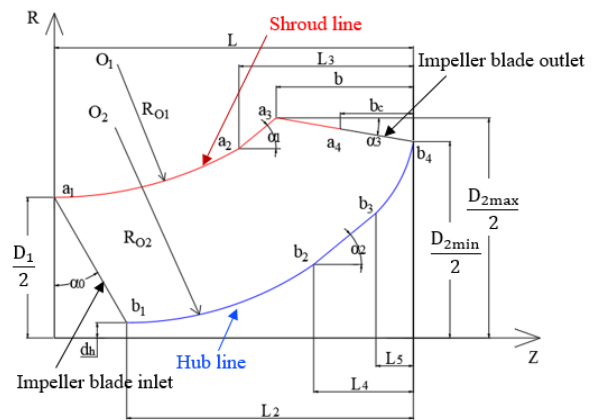


Fig. 2 Meridional plane shape of screw centrifugal impeller blade model (initial model)

Table 2 Design parameters of meridional shape of the pump impeller (initial model)

Item	Nomenclature (1)	Range	Initial value
Impeller outlet diameter	$D_{2max} [mm]$		360
Coefficient of impeller outlet diameter	$K_{D_2}$	10.5~12.5	11.5
Hub diameter	$D_{2min} [mm]$		321.21
Impeller inlet diameter	$D_1 [mm]$		230
Coefficient of impeller inlet diameter	$K_{D_1}$	4.5~6.5	5
Shaft diameter	$d_h [mm]$		25
Outlet width	$b [mm]$		110
Total axial length	$L [mm]$		288
Coefficient of total axial length	$K_L$	0.6~1	0.8
Hub axial length	$L_2 [mm]$		230
Inclination angle 1	$\alpha_1 [^\circ]$		40
Inclination angle 2	$\alpha_2 [^\circ]$		40
Blade inlet angle	$\alpha_0 [^\circ]$		25
Blade outlet angle	$\alpha_3 [^\circ]$		10

specifically, the spiral profile of the blade. The  $Z$ -axis and  $R$ -axis are used instead of the  $x$ -axis and  $y$ -axis, where  $Z$  is the axial length and  $R$  is the radius. The starting points of shroud line and hub line rotates around the  $Z$ -axis with a fixed angular velocity ( $\omega_i$ ), and moves along the positive direction of  $Z$ -axis at an axial velocity ( $v_i$ ) on the surface ( $R=f(z)$ ).

The profile equations of shroud line are defined as follows;

$$\theta_s = 3900 \cdot t_s \quad (1)$$

$$Z_s = 1538 \cdot t_s \quad (2)$$

$$\begin{aligned} R_s &= 409.9 - \sqrt[3]{294.9^2 - Z_s^2} & (0 \leq Z_s [mm] \leq 148) \\ &= 180 - (178 - Z_s) \tan 40 & (148 \leq Z_s [mm] \leq 178) \\ &= 180 - (Z_s - 178) \tan 10 & (178 \leq Z_s [mm] \leq 229) \end{aligned} \quad (3)$$

The profile equations of hub line are defined as follows;

$$\theta_h = 3900 \cdot t_h \quad (4)$$

$$Z_h = 1538 \cdot t_h + 58 \quad (5)$$

$$\begin{aligned} R_h &= 272.67 - \sqrt[3]{260.17^2 - (Z_h - 58)^2} & (58 \leq Z_h [mm] \leq 208) \\ &= 60.1 + (Z_h - 208) \tan 40 & (208 \leq Z_h [mm] \leq 258) \\ &= 180 - \sqrt[3]{111.7^2 - (Z_h - 178)^2} & (258 \leq Z_h [mm] \leq 288) \end{aligned} \quad (6)$$

where  $\theta$ ,  $Z$ ,  $R$  and  $t$  represent the wrap angle of impeller blade, the length in the  $Z$ -axial direction, the blade radius and the equation variable, respectively,  $s$  is the shroud line and  $h$  is the hub line.

The shroud and hub profiles are drawn according to Eqs. 1 to 6 as shown in Fig. 3. The total wrap angles of the shroud line and hub line are  $581^\circ$  and  $583^\circ$ , respectively, and the total wrap angle of the centrifugal part is  $130^\circ$ . The 3D modeling of the screw centrifugal pump impeller initial model is shown in Fig. 4. The spiral casing of the screw centrifugal pump is designed as the normal centrifugal pump casing design process with the circular shape of casing cross-section<sup>(10)</sup>.

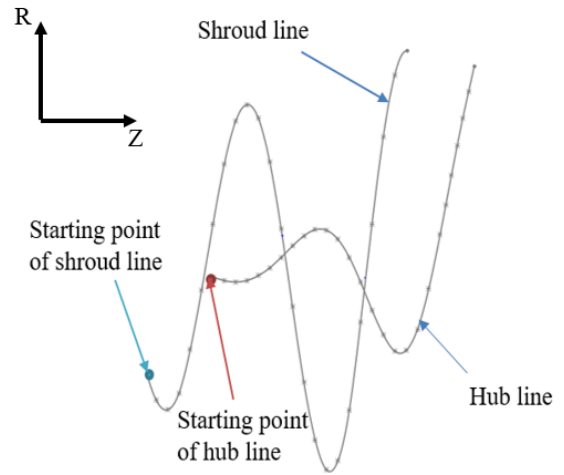


Fig. 3 Shroud and hub profile lines for the pump impeller initial model

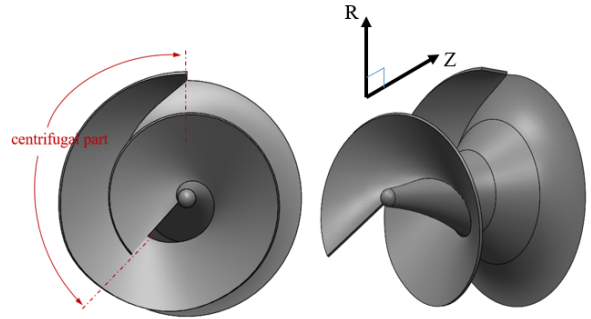


Fig. 4 3D modeling of screw centrifugal pump impeller initial model

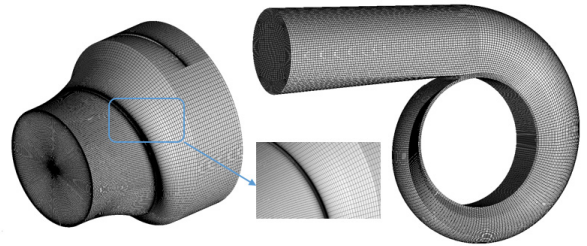


Fig. 5 Numerical grids of impeller and volute casing fluid domains for the pump initial model

### 3. Numerical Method

The fluid domain of the screw centrifugal pump geometry was modeled in 3D. CFD analysis was conducted by using a commercial code of ANSYS CFX 18.1. The hexahedral mesh was generated by ANSYS ICEM 18.1<sup>(11)</sup>. Fig. 5 illustrates the numerical grids of impeller and volute casing fluid domains for the pump initial model. Moreover, the mesh dependence test for

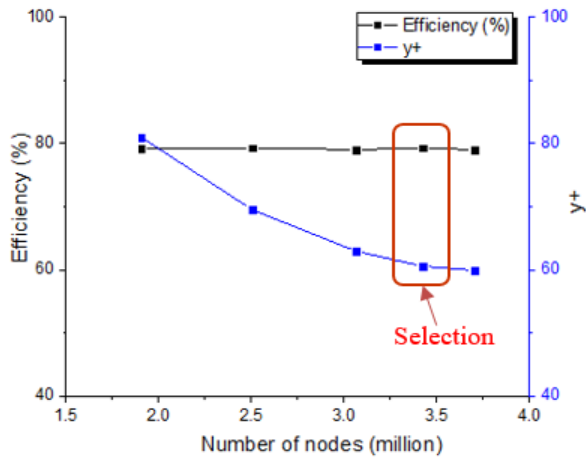


Fig. 6 Mesh dependence test for the pump initial model

the pump initial model is implemented as shown in Fig. 6. The mesh dependence test is conducted by investigating the stability of the efficiency and the  $y+$  value calculated by using Eqs. 7 and 8.

$$\eta = \frac{\rho g H Q}{\tau \omega} \quad (7)$$

$$y+ = \frac{y U_T}{\nu} \quad (8)$$

where  $\rho, g, H, Q, \tau$  and  $\omega$  stand for the density of water, acceleration of gravity, head, flow rate, torque and angular velocity, respectively.  $y, U_T$  and  $\nu$  are the absolute distance from the wall, the friction velocity and the kinematic viscosity, respectively.

The structure of the screw centrifugal pump impeller is quite complex, so the  $y+$  value of the impeller was set to 60 at the maximum value. Finally, a mesh number of 3.4 million nodes is selected to conduct the CFD analysis for the screw centrifugal pump model. The information of the numerical grids is shown in detail in Table 3.

The turbulence models of  $k-\epsilon$ ,  $RNG k-\epsilon$ , and  $SST$  are used to conduct the turbulence model dependence test, and the test results are presented in Fig. 7. As the  $SST$  turbulence model is well known for estimating both separation and swirling flow on the wall of complex blade shapes, reasonably, the  $SST$  turbulence model is employed for CFD analysis in this study. The whole numerical analysis study was conducted by the Workstation computer with the specifications Intel(R)

Table 3 Information of numerical grids for the pump initial model

	Node number	Element number
Impeller	1,947,665	1,522,936
Volute	357,022	194,390
Inlet pipe	302,880	293,335
Outlet pipe	302,880	293,335
Total	3,428,465	3,303,533

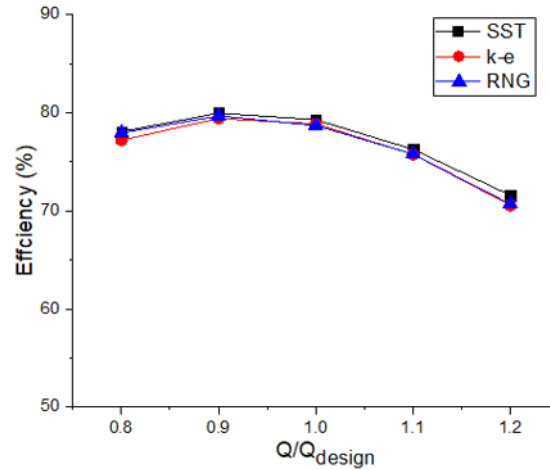


Fig. 7 Turbulence model dependence test for the pump initial model

Table 4 Numerical method and boundary condition

Analysis type	Steady state
Working fluid	Water at 25°C
Inlet	Mass flow rate
Outlet	Static pressure
Turbulence model	Shear Stress Transport ( $SST$ )
Walls	No slip wall

Xeon(R) CPU E5-2640 0 @ 2,5GHz 2,5GHz (2 processors), 48GB RAM, 64-bit Operating System, x64-based processor for almost 10 weeks.

The numerical method and boundary conditions for steady state analysis are illustrated in Table 4. The mass flow rate and static pressure are set for the inlet and outlet boundary conditions of the pump, respectively. The general connection is set as a frozen rotor between the fixed domain and the rotational domain.

## 4. Results and Discussion

### 4.1 Performance curves by a pump initial model

The performance curves by a pump initial model are

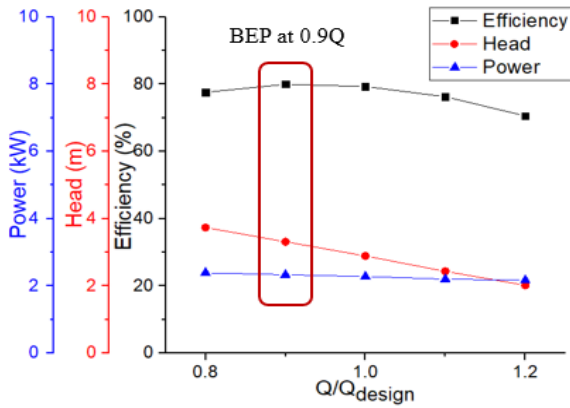


Fig. 8 Performance curves of a screw centrifugal pump initial model

presented in Fig. 8. The parameters of the initial model shown in Table 2 were selected from the middle value range of the equations referred to<sup>(1,7)</sup>. Therefore, it is conjectured that a few of parameters is not suitable with the specification design and the initial model is quite small that makes the position problem of BEP. So, after the various values of parameters on the impeller meridional plane shape are investigated their impacts on the performance curves, the new parameters are selected for the base model which the BEP matches well with design point ( $Q/Q_{design} = 1.0$ ).

#### 4.2 Effect of impeller meridional plane shapes on the pump performance

The impeller meridional plane shape is determined by the flow rate and effective head of the screw

Table 5 The ranges of design parameters for impeller meridional plane shape investigation

Design parameters							
$K_{D1}$	$\alpha_0 [^\circ]$	$\alpha_3 [^\circ]$	$\alpha_1 [^\circ]$	$\alpha_2 [^\circ]$	$K_{D2}$	$b [mm]$	$K_L$
5~6.25	25	10	40	40	11.5	110	0.8
6	0~42	10	40	40	11.5	110	0.8
6	25	0~20	40	40	11.5	110	0.8
6	25	10	35~45	40	11.5	110	0.8
6	25	10	40	35~45	11.5	110	0.8
6	25	10	40	40	11.5~12.5	110	0.8
6	25	10	40	40	12	110~130	0.8
6	25	10	40	40	12	120	0.6~1

centrifugal pump. The design parameters of the impeller meridional plane shape are the impeller inlet and outlet diameters, blade inlet and outlet angles, outlet width, total axial length, and inclination angles. The variation in the design parameters leads to a change in the impeller meridional plane shape. For the initial model, the parameters change one by one to study their influence on the pump performance. The conditions for the selection of the new parameters are the head and efficiency improvement as well as its BEP position matching with the design point. Table 5 shows the ranges of design parameters to investigate the change in pump performance.

##### 4.2.1 Effect of impeller inlet diameter

The coefficient of impeller inlet diameter  $K_{D1}$  is used to calculate the inlet diameter of impeller. Design parameter range of the impeller inlet diameter are shown in Table 5. Fig. 9 shows the performance curves of the screw centrifugal pump for various  $K_{D1}$ . Fig. 9 indicates that the head at the design point increases with an increase in inlet diameter, but the efficiency decreases accordingly, thus,  $K_{D1} = 6$  is selected as a base model parameter of the pump performance optimization.

##### 4.2.2 Effect of impeller blade inlet and outlet angles

The design variable ranges of the various impeller blade inlet angle  $\alpha_0$  and blade outlet angle  $\alpha_3$  are illustrated in Table 5. Fig. 10 shows the influence of the impeller blade inlet angle on pump performance. As the impeller blade inlet angle increases from  $0^\circ$  to  $42^\circ$ , at the design point, the value of the pump efficiency increases, and the head decreases.

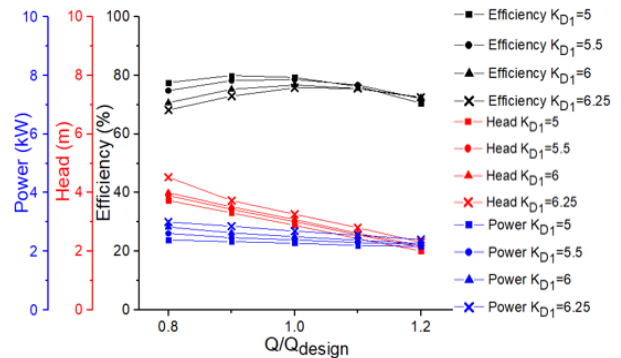


Fig. 9 Effect of impeller inlet diameter

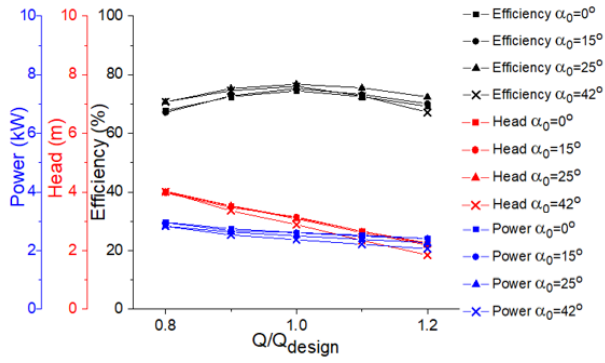


Fig. 10 Effect of impeller blade inlet angle

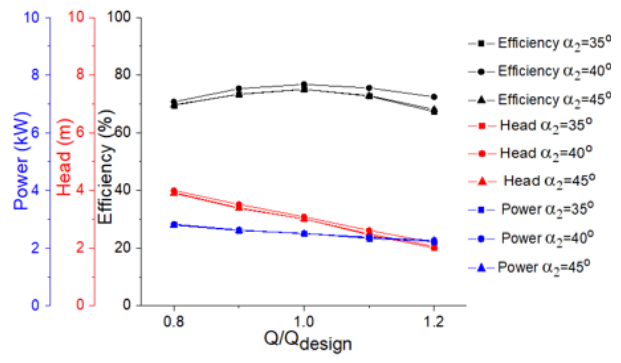


Fig. 13 Effect of impeller blade inclination angle  $\alpha_2$

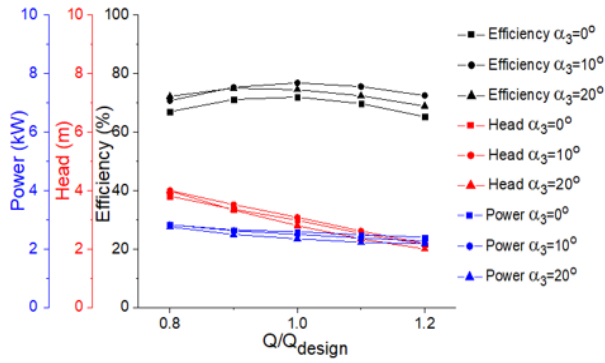


Fig. 11 Effect of impeller blade outlet angle

The results of performance curves by the impeller blade outlet angle in Fig. 11 indicate that the case of  $\alpha_3 = 10^\circ$  is the most efficient compared with the others. Finally,  $\alpha_0 = 25^\circ$  and  $\alpha_3 = 10^\circ$  are selected as base model parameters for the optimum design.

#### 4.2.3 Effect of impeller blade inclination angles

The design variable ranges of impeller blade inclination angles  $\alpha_1$  and  $\alpha_2$  are shown in Table 5. Three cases of  $\alpha_1$  and  $\alpha_2$  are  $35^\circ, 40^\circ$  and  $45^\circ$ . Figs. 12 and 13 indicate the performance curves by the various  $\alpha_1$  and  $\alpha_2$ . The results by the various  $\alpha_1$  and  $\alpha_2$  show

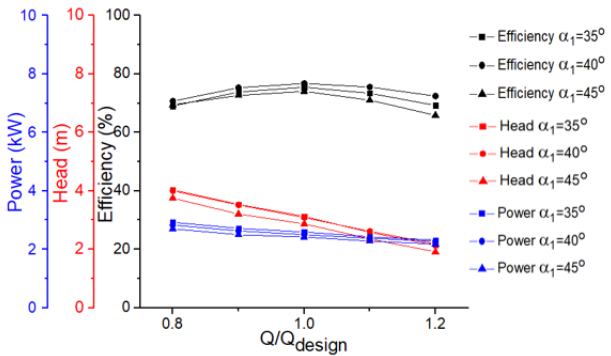


Fig. 12 Effect of impeller blade inclination angle  $\alpha_1$

that  $\alpha_1 = 40^\circ$  and  $\alpha_2 = 40^\circ$  have the better pump efficiency compared with the others. Therefore,  $\alpha_1 = 40^\circ$  and  $\alpha_2 = 40^\circ$  are selected as base model parameters.

#### 4.2.4 Effect of impeller outlet diameter

The coefficient of impeller outlet diameter  $K_{D_2}$  is used to calculate the outlet diameter of impeller. The design variable ranges of the impeller outlet diameter coefficient are shown in Table 5. Fig. 14 shows the performance curves of the screw centrifugal pump for various  $K_{D_2}$ . When the impeller outlet diameter increases, the BEP moves to a higher flow rate, for instance, with  $K_{D_2} = 11.5$  and 12, the BEP at the design point, and with  $K_{D_2} = 12.5$ , the BEP at  $1.1 Q_{design}$ . As the impeller outlet diameter increases, the head increases because the outlet circumferential velocity increases, and eventually, the outlet pressure increases. With  $K_{D_2} = 12$ , the head and efficiency are better than case  $K_{D_2} = 11.5$ , and the BEP matches well with the design flow rate, whereas  $K_{D_2} = 12.5$ , BEP is at  $1.1 Q_{design}$ , therefore,  $K_{D_2} = 12$  is selected as a base model parameter.

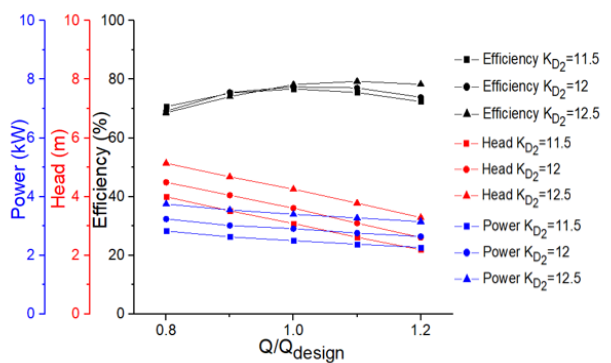


Fig. 14 Effect of impeller outlet diameter

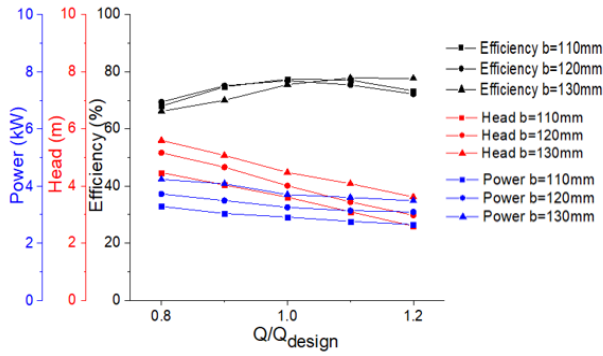


Fig. 15 Effect of impeller outlet width

#### 4.2.5 Effect of impeller outlet width

The various impeller outlet widths  $b$  from 110mm to 130mm are selected to study the effect of impeller meridional plane shape on the pump performance as shown in Fig. 15. The results implies that the outlet width plays an essential role in the determination of the head of the screw centrifugal pump. At the design point, the increase of the impeller outlet width decreases the pump efficiency and increases the pump head. For the increasing impeller outlet diameter, the BEP moves to the higher flow rate range,  $b = 120$ mm is selected as a base model parameter, because the head of case  $b = 120$ mm is higher than case  $b = 110$ mm, and the BEP is at the design point, whereas case  $b = 130$ mm, BEP is at  $1.1 Q_{design}$ .

#### 4.2.6 Effect of impeller total axial length

According to the previous study<sup>(1,7)</sup>, the total axial length depends on the impeller outlet diameter. In the industry, this coefficient can be selected more than 1. However, the larger coefficient of total axial length can cause the problem on the pump rotating shaft, so in this study, the various values of the

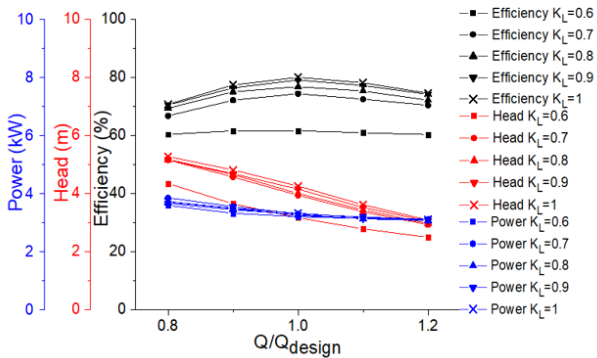


Fig. 16 Effect of impeller total axial length

impeller total axial length coefficient  $K_L$  were selected from 0.6 to 1, Fig. 16 indicates the effect of impeller total axial length on the pump performance. The increase of the impeller total axial length has a remarkable influence on the pump performance, the pump efficiency and head are improved significantly. Therefore, the impeller total axial length is considered as an important design parameters for the screw centrifugal pump.  $K_L = 1$  is selected as a base model parameter.

#### 4.3 Optimization process

The optimization flowchart for the improvement of the pump efficiency is shown in Fig. 17. According to the parametric study, the best design parameters were selected for the design of the base model. The purpose of optimization is to improve the efficiency of the screw centrifugal pump. The design of experiments (DOE) is created by the orthogonal array method<sup>(12)</sup> and evaluated by using numerical analysis. The numerical analysis results were used to construct the surrogate model. The surrogate model is used to conduct the optimization by using an Evolutionary Algorithm<sup>(13)</sup>. The optimization procedure is carried out on the commercial software of ANSYS OptiSlang<sup>(14)</sup>.

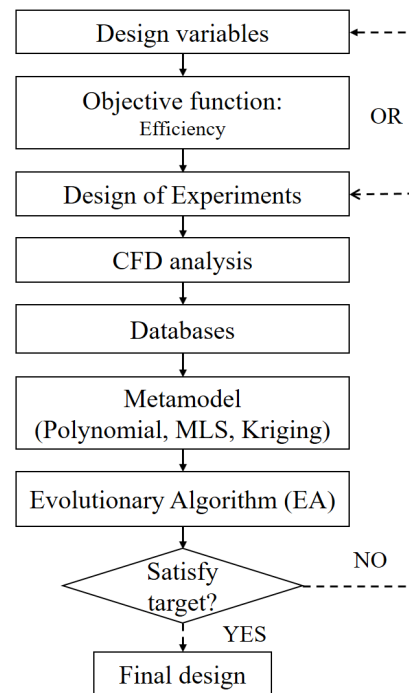


Fig. 17 The optimization process of screw centrifugal pump

Table 6 Design parameters of a base model impeller meridional plane shape

Inlet diameter coefficient ( $K_{D_1}$ )	6	Inclination angle 1 ( $\alpha_1 [^\circ]$ )	40
Outlet diameter coefficient ( $K_{D_2}$ )	12	Inclination angle 2 ( $\alpha_2 [^\circ]$ )	40
Outlet width ( $b [mm]$ )	120	Blade outlet angle ( $\alpha_3 [^\circ]$ )	10
Total axial length coefficient ( $K_L$ )	1	Blade inlet angle ( $\alpha_0 [^\circ]$ )	25

4.3.1 Base model

According to the parametric study, the values of parameter are selected to generate the base model. The detailed design parameters of the base model are shown in Table 6. The impeller meridional plane shape and the pump performance curves of the base model are illustrated in Figs. 18 and 19, respectively. The BEP and the design point of the base model match

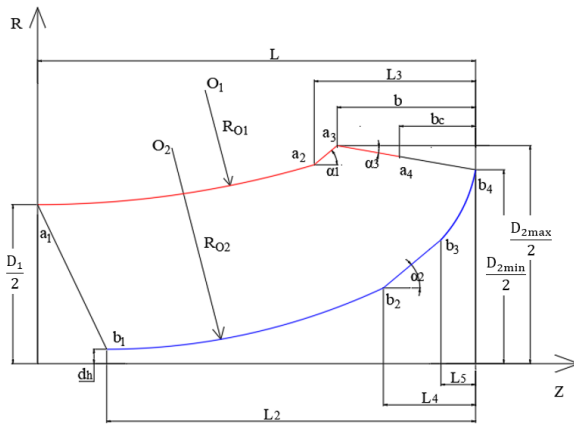


Fig. 18 Impeller meridional plane shape of base model

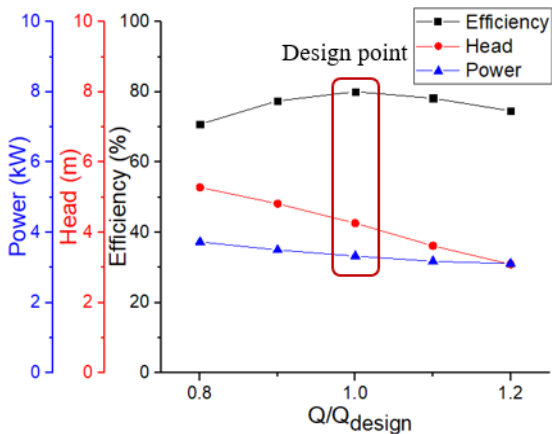


Fig. 19 Pump performance curves of base model

well. The base model is used for the pump efficiency optimization. The parameters, such as impeller inlet diameter, total axial length, inclination angles, and blade inlet angle are selected as design variables to optimize the impeller meridional plane shape. These parameters not only show the effective influence on the pump performance, but also have the BEP location matching well with the design point. Whereas the slightly changing of the impeller outlet diameter, outlet width and blade outlet angle can distort the BEP position. Therefore, three design parameters are fixed in the optimization study.

4.3.2 Objective function

In this study, the optimization is carried out to improve the hydraulic pump performance, specifically, to maximize efficiency, which is defined as shown in Eq. 7.

4.3.3 Design variables

Design variables of parameters are selected such as  $K_{D_1}$ ,  $K_L$ ,  $\alpha_0$ ,  $\alpha_1$ ,  $\alpha_2$  to make the design of experiments. The orthogonal array method<sup>(12)</sup> is used to identify the sensitivity of design variables for objective function in this study.

The range of design variables is set as follows:

$$5.25 \leq K_{D_1} \leq 6.25 \tag{9}$$

$$0.8 \leq K_L \leq 1 \tag{10}$$

$$0 \leq \alpha_0 \leq 40 \tag{11}$$

$$30 \leq \alpha_1 \leq 50 \tag{12}$$

$$30 \leq \alpha_2 \leq 50 \tag{13}$$

Table 7 shows DOE created by using the orthogonal array method and their CFD analysis results. The sensitivity analysis is applied to identify the influence of the design variables on the objective function. The sum values of each level for each design variable are defined as  $K_i$  and the averaged values are defined as  $\bar{K}_i$ . The value of  $K_i$  and  $\bar{K}_i$  are calculated using equations as follows:



Table 7 Numerical analysis results of DOE

No.	$K_{D_1}$	$K_L$	$\alpha_1 [^\circ]$	$\alpha_2 [^\circ]$	$\alpha_0 [^\circ]$	$\eta[\%]$
1	5.25	0.8	30	30	0	76.78
2	5.25	0.85	35	35	10	79.61
3	5.25	0.9	40	40	20	80.98
4	5.25	0.95	45	45	30	80.74
5	5.25	1	50	50	40	79.57
6	5.5	0.8	35	40	30	80.25
7	5.5	0.85	40	45	40	80.55
8	5.5	0.9	45	50	0	79.37
9	5.5	0.95	50	30	10	78.76
10	5.5	1	30	35	20	82.98
11	5.75	0.8	40	50	10	77.97
12	5.75	0.85	45	30	20	78.64
13	5.75	0.9	50	35	30	79.78
14	5.75	0.95	30	40	40	82.38
15	5.75	1	35	45	0	80.90
16	6	0.8	45	35	40	78.40
17	6	0.85	50	40	0	77.18
18	6	0.9	30	45	10	79.80
19	6	0.95	35	50	20	81.21
20	6	1	40	30	30	81.85
21	6.25	0.8	50	45	20	75.61
22	6.25	0.85	30	50	30	79.50
23	6.25	0.9	35	30	40	80.54
24	6.25	0.95	40	35	0	77.06
25	6.25	1	45	40	10	78.84

$$K_i = \sum_{j=1}^i Y_{ij} \quad (14)$$

$$\bar{K}_i = \frac{1}{i} K_i \quad (15)$$

where  $i$  is the number of the level,  $j$  is the number of the design variable,  $Y_{ij}$  is the value of objective, which corresponds to the design variable  $j$  in the level  $i$ ,  $\Delta$  is equal to difference between maximum and minimum values of the objective.

Table 8 and Fig. 20 show the sensitivity analysis of the effect of design parameters on the pump efficiency. According to the sensitivity analysis,  $K_L$ ,  $\alpha_1 [^\circ]$ ,  $\alpha_0 [^\circ]$ ,  $K_{D_1}$  and  $\alpha_2 [^\circ]$  are arranged from the most sensitive to the least. The total axial length coefficient ( $K_L$ ) is the most important design variable for the pump efficiency improvement.

Table 8 Sensitivity analysis

Values	Design parameters				
	$K_{D_1}$	$K_L$	$\alpha_1 [^\circ]$	$\alpha_2 [^\circ]$	$\alpha_0 [^\circ]$
$K_1$	397.69	389.02	401.44	396.57	391.30
$K_2$	401.91	395.48	402.52	397.83	394.97
$K_3$	399.67	400.47	398.41	399.63	399.41
$K_4$	398.44	400.16	395.99	397.60	402.12
$K_5$	391.56	404.16	390.92	397.65	401.47
$\bar{K}_1$	79.54	77.80	80.29	79.31	78.26
$\bar{K}_2$	80.38	79.10	80.50	79.57	78.99
$\bar{K}_3$	79.93	80.09	79.68	79.93	79.88
$\bar{K}_4$	79.69	80.03	79.20	79.52	80.42
$\bar{K}_5$	78.31	80.83	78.18	79.53	80.29
$\Delta$	2.07	3.03	2.32	0.61	2.16
Rank	4	1	2	5	3

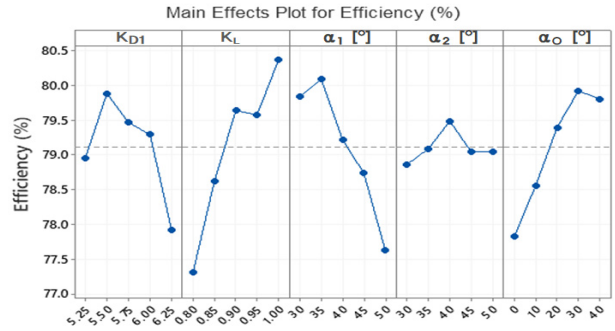


Fig. 20 Plot of influence of design parameters on the pump efficiency

#### 4.3.4 Optimized results

The surrogate model is prepared by the combination of polynomial regression, moving least square and Kriging. Polynomial regression<sup>(15)</sup> is a common approximation method where the output response is generally approximated by a polynomial basis function of linear or quadratic order equation with or without coupling terms showed in Eqs. 16 and 17.

$$y_i = \beta_0 + \sum_{i=1}^k \beta_i x_i + \epsilon_i \quad (16)$$

$$y_i = \beta_0 + \sum_{i=1}^k \beta_i x_i + \sum_{i=1}^k \beta_{ii} x_i^2 + \sum_{i=1}^k \sum_{j=1, i < j}^k \beta_{ij} x_i x_j + \epsilon_i \quad (17)$$

where  $y_i$  is the model output,  $x_i$  is the input

parameter,  $\beta_i$  is the coefficient of the equation and an error term  $\varepsilon_i$ .

Moving Least Square (MLS)<sup>(15)</sup> is a local approximation method of the regression as an extension of the polynomial regression. Kriging<sup>(13)</sup> is the local approximation method that maximize the likelihood function to find optimal parameters. MLS and Kriging are employed to find the approximate relationship between input variables and output target.

The Evolutionary Algorithm<sup>(13)</sup> is used to conduct the optimization on the impeller meridional plane shape.

Fig. 21 illustrates the comparison of the impeller meridional plane shapes by the initial, base and optimum models. The comparison of design parameters between the base model and the optimum model is shown in Table 9. The numerical analysis indicated that the efficiency of the optimum model is 82.43% that drops by 0.65% compared with the optimal model predicted by surrogate model.

Fig. 22 indicates that the efficiency of the optimum model is higher than the base model at a wide operating range. At the design point, the efficiency of the optimum model is increased by 2.35%.

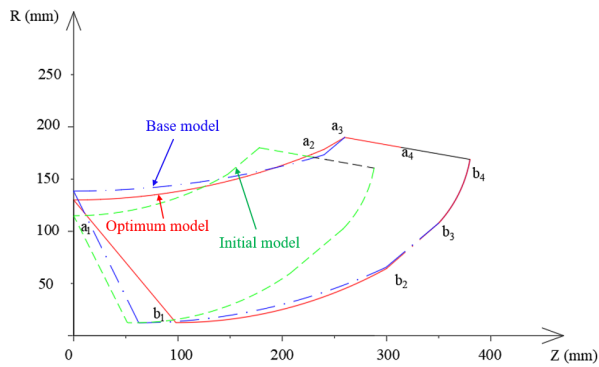


Fig. 21 Comparison of impeller meridional plane shapes

Table 9 Comparison of design parameters by the base and optimum models by CFD analysis

Design parameters	Base model	Optimum model
$K_{D1}$	6	5.63
$K_L$	1	1
$\alpha_1(^{\circ})$	40	30
$\alpha_2(^{\circ})$	40	41.2
$\alpha_0(^{\circ})$	25	39.9
Efficiency (%)	80.08	82.43

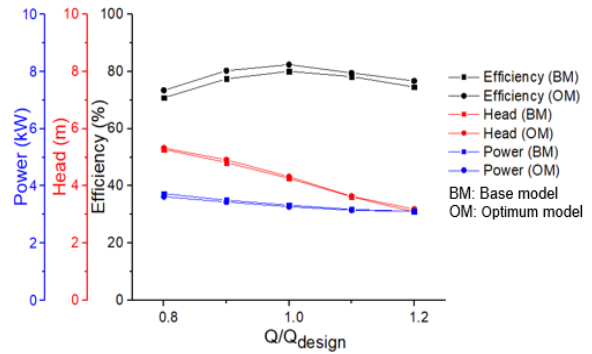


Fig. 22 Comparison of performance curves between the initial, base and optimum models (CFD analysis results)

## 5. Conclusions

The aim of this study is focused on the optimization of the impeller meridional plane shape design parameters of a screw centrifugal pump to improve the pump performance, especially the pump efficiency.

The total process of the pump efficiency optimization is figured out and conducted to investigate the effect of the various impeller meridional plane shape design parameters of the screw centrifugal pump on the pump performance as follows;

1. Design method establishment based on the blade profile equations.
2. Initial model determination for the design method verification.
3. Base model determination to match the design specification.
4. Optimum model determination to improve the pump efficiency.

The initial model is used to investigate the design parameters, which include the impeller inlet and outlet diameters, blade inlet and outlet angles, outlet width, total axial length, and inclination angles. From the investigation of the design parameters of the initial model, reasonable values of the parameters are selected to generate the base model which has the pump performance matching well with the design specification. The base model is applied for the optimum design to improve the pump efficiency.

The study results show that the impeller outlet diameter and total axial length are confirmed as the most important parameters among the investigated parameters to improve the pump performance. The

pump efficiency of the optimum model is 82.43% at the design point, which is 2.35% higher than the base model.

## References

- (1) Guan, X. F., 2011, Modern pump theory and design, China Astronaut, Beijing, China (in Chinese).
- (2) Kim, Y., Tanaka, K., Lee, Y., Matsumoto, Y., 1999, "Effects of entrained air on the characteristics of a small screw-type centrifugal pump", The KSFM Journal of Fluid Machinery, Vol. 2, No. 3, pp. 37~44.
- (3) Tatebayashi, Y., Tanaka, K., 2002 "Influence of meridional shape on screw-type centrifugal pump performance". Proc. of ASME Fluids Engineering Division Summer Meeting, FEDSM2002-31183, pp. 769~776, Canada.
- (4) Tatebayashi, Y., Tanaka, K., Kobayashi, T., 2003, "Thrust prediction in screw-type centrifugal pump". Proc. of 4th ASME\_JSME Joint Fluid Engineering Conference, FEDSM2003-45105, pp. 621~626, Hawaii, USA.
- (5) Tatebayashi, Y., Tanaka, K., Kobayashi, T., 2005 "Pump performance improvement by restraining back flow in screw-type centrifugal pump". ASME Journal of Turbomachinery, pp. 755~762, Houston, TX, USA.
- (6) Cheng, X., Lia, R., 2012, "Parameter equation study for screw centrifugal pump". Procedia Engineering, Vol. 31, pp. 914~921.
- (7) Guo, M., Choi, Y. D., 2017, "Design and CFD analysis of a screw centrifugal pump model". Journal of the Korean Society of Marine Engineering, Vol 43, No. 8, pp. 640~647.
- (8) ANSYS Inc, ANSYS CFX Documentation, Ver. 18.1, <http://www.ansys.com>, Accessed, 2018.
- (9) Min, Z., Zhu, D, K., Han, W., Zhang, Z. H., Li, Z. Y., 2012, "Improvement of hydraulic design method for screw centrifugal pump impeller based on auxiliary lines". Journal of Lanzhou University of Technology, Vol. 38, No. 2, pp. 47~50 (in Chinese).
- (10) Stepanoff, A. J., 1957, Centrifugal and Axial Flow Pumps: Theory, Design, and Application, 2<sup>nd</sup> edition, John Wiley & Sons, Inc.
- (11) ANSYS ICEM., ANSYS ICEM Documentation, Ver. 18.1, <http://www.ansys.com>, Accessed, 2018.
- (12) Taguchi, G., Wu, Y., 1985, Introduction to off-line quality control, Central Japan Quality Control Association, Tokyo.
- (13) Kim, K. Y., Samad, A., Benini, E., 2019, Design Optimization of Fluid Machinery: Applying Computational Fluid Dynamics and Numerical Optimization, John Wiley & Sons Singapore Pte. Ltd.
- (14) ANSYS OptiSLang., ANSYS optiSLang Doc., Ver. 18.1, <http://www.ansys.com>, Accessed, 2018.
- (15) Most, T., Will, J., 2011, "Sensitivity analysis using the Metamodel of Optimal Prognosis", Weimar Optimization and Stochastic Days, 8, pp. 24~40.